

## Research Article

# Green Synthesis of Calcium/Iron-Layered Double Hydroxides-Sodium Alginate Nanoadsorbent as Reactive Barrier for Antibiotic Amoxicillin Removal from Groundwater

Marwa F. Abed  and Ayad A. H. Faisal 

Department of Environmental Engineering, College of Engineering, University of Baghdad, Baghdad, Iraq

Correspondence should be addressed to Marwa F. Abed; marwaspider@gmail.com

Received 24 July 2022; Revised 4 January 2023; Accepted 28 March 2023; Published 17 April 2023

Academic Editor: Muhammad Raziq Rahimi Kooh

Copyright © 2023 Marwa F. Abed and Ayad A. H. Faisal. This is an open access article distributed under the Creative Commons Attribution License, which permits unrestricted use, distribution, and reproduction in any medium, provided the original work is properly cited.

This work uses a new nanoadsorbent after chemically synthesis from chicken eggshell wastes for removing amoxicillin (AMX) from aqueous solution. This removal was examined as a time function, initial concentration of AMX, pH, agitation speed, and adsorbent dosage. The study achieved the optimum time for equilibration in (90) min, at pH = 7 with an adsorbent dosage of 1.2 g. We applied many kinetic models to the sorption kinetic data where the pseudo-second-order model ( $R^2 = 0.9924$ ) was used to interpret the gained data at a rate constant  $K_2$  of (0.0077) g/(mg. min) at 200 rpm. Moreover, the adsorption calculated amount reached the experimentally required value and isotherm data best fitted the Langmuir model with  $R^2$  ( $\geq 0.9486$ ) than the Freundlich model. The intraparticle diffusion model revealed a diffusion dependent process. The different functional sets on the calcium/iron-surface as a layered double hydroxide (Ca/Fe)-LDH were important in sorption the selected antibiotic. Forming (Ca/Fe)-LDH nanoparticles in the manufactured beads interacted with polluted water confirming that the nanoparticles own the prospective for acting as a latent sorbent to remove contaminants from aquatic media.

## 1. Introduction

A very significant natural resource is groundwater to both terrestrial and aquatic ecosystems. One third of the world's population drinks groundwater as their primary potable source and uses it for domestic, production of food, industry [1], and irrigation of 40% of the food worldwide [2], despite its limited ecological resources consisting of a small portion of the total water distribution [3, 4]. While the standards and needs of living on our natural environment are expanding, rising populations, ongoing urbanization, and industry increase the risk of groundwater contamination [5]. In addition, numerous reports showed dangerous groundwater contamination caused by accidental spills, unsafe disposing industrial chemicals, agricultural practices, mining, etc. Contaminants are dangerous to human health. They also make natural ecosystems vulnerable, and the same is true with the long-term socioeconomic [6] including toxic metals

and hydrocarbons. In addition, the organic trace pollutants, pharmaceutical polluting elements, and pesticides face the same, and if managed improperly, groundwater reservation can result in the release of these pollutants into the environment [7, 8]. Antibiotics are one of the most commonly used classes of pharmaceutical compounds, and they are perhaps the most effective class of drugs ever created for enhancing human health. They also prevent and treat animal and plant infections and raise productivity in the livestock industry [9]. Its use is expected to be on the order of 100 000 to 200 000 tons per year throughout the world [10]. Yet, the World Health Organization [11] claimed that only some nations possess national statistics of the antibiotic usage, quantities, and patterns. As a result, the quantity of antibiotics consumed is not clear. Its main sources are human and animal incompletely metabolized antibiotics in the environment. Since humans excrete a large portion of their antibiotics in the form of feces or urine, as well as through disposing

leftover hospital antibiotics and wastes, antibiotics are ubiquitous in nature, and their residues have frequently been found in various environmental matrices [12, 13]. AMX was first made available for human use in the early 1970s in the United Kingdom. Since then, it has been discovered in a variety of water bodies due to its widespread use to resist many gram-positive and -negative microorganisms and its status as a first-line antibiotic in numerous nations [14]. Beside the human medicine use, amoxicillin treats and prevents animal infections for increasing growth in a variety of domestic and food animals for broiler chickens, dogs, cats, horses, pigeons, pigs, sheep, goats, preruminating calves, cattle, and fish [15]. Usually, amoxicillin environmental degradation by a number of processes, such as (1) sorption, (2) transformation in biotics, and (3) transformation in abiotics, can influence the destiny and transit of organic compounds in the environment [16]. Over the years, the developments of treatment technologies and approaches for contaminated groundwater have become available allowing flexibility in how clean-up goals can be achieved. Permeable reactive barriers (PRBs) as treatments, depending on sorption process since it removes groundwater contaminants, have been widely examined [17]. It has to be reactive. In addition, it has permeability bigger or equal to the ambient aquifer; thus, the right material choice for the barriers is important [18]. The previous research focused on using wastes, recycled, and by-product materials in PRB technology to enhance their activity in using sustainable (green) concepts, such as activated neem leaves [19], coir pith [20], recycled concrete [21], municipal composts, leaf composts, wood chips, limestone, silica sand [22], and peat and sawdust [23] in treating water contaminated with pollutants. Eggs represent as one of the most ingredient used in variety of products resulting in several daily tons of eggshell which is ranked as the 15th major food industry pollution problem by the EPA, and most of these quantities are accumulated on site or disposed annually as waste in landfills without any pretreatment and become as an organic environmental pollution source [24]. Furthermore, with increasing urgent recently to converting worthwhile waste into useful commodities for sustainable development by recycle, reuse for manufacturing high-value products, managing agricultural wastes is vital and a crucial strategy [25]. Eggshells are one such agrowaste that can be used as a useful source of material in a variety of applications, including the manufacturing of fertilizer and feed as well as other environmentally friendly catalysts in biological, environmental, and agricultural engineering applications [26]. The structural aspect of eggshell comprises of calcium carbonate as the main component with (94-95%) [27], so utilizing eggshells can provide biocompatible calcium (it is environmentally friendly and nontoxic) which lowers not only the impact of pollution but also the associated financial costs and serves as a commercial replacement for calcium carbonate, calcium hydroxide, and calcium oxide [28], and it is also utilized for fertilization, soil conditioning, or animal feed ingredients [29] and manufacturing food products including calcium additives [30]. Layered double hydroxides (LDHs) are unique in structure which is a two-dimensional structure in which the cations are in the

centers of edge-sharing octahedral, with vertexes containing OH ions connecting and constituting infinite 2D sheets as [31], with high positive charge densities of layers and high contents of interlayer anionic species which result in strong electrostatic interactions that made the layers hold together in LDHs beside the hydrogen bond [32]. LDHs are active adsorbents, so most scholars have synthesized many LDHs to remove antibiotics from wastewater [33], additionally, and it is prepared relatively simply and economically through a coprecipitation method under laboratory setting in big quantities [34]. The previous studies concentrated on the using of LDHs for antibiotics removal such as in [35] adsorption of AMX that was studied were performed on *Cladophora* and *Spirulina* algae biomass immobilized in alginate beads in batch mode with algal biomass doses of 1.25 g/100 ml and 0.5 g/100 ml in respect, achieving 98% of removal, and maximal adsorption capacity was 7.89, 17.4 mg/g for AMX, while Yang et al. [36] studied synthesis as novel adsorbents Mg-Al LDH/cellulose nanocomposite beads (LDH@CB) by coprecipitation procedure utilized as a new adsorbent to remove AMX from the aqueous solution in kinetically and isothermally batch adsorption experiment and fitted with the Freundlich isotherm and pseudo-second-order model, respectively, and AMX LDH@CB qm adsorption capacity equals 138.3 mg g<sup>-1</sup>. Elhaci et al. [37] also investigated the LDH material synthesis by Mg<sup>2+</sup>/Al<sup>3+</sup> molar rate of 2 by coprecipitation at pH 9 to remove AMX from aqueous media by pseudo-second-order kinetics with highest adsorption monolayer capacity recorded at pH = 6, with 30.42 mg/g at C<sub>0</sub> = 240 mg/L. This work is aimed at using the eggshell wastes usefully for sustainable development by extracting calcium ions from eggshell wastes to synthesis (Ca/Fe)-LDH nanoabsorbent and entrapped in sodium alginate beads to forming (Ca/Fe)-LDH-sodium alginate beads or (Ca/Fe)-LDH-SA beads for AMX removal with finding the optimal operation parameters and implement this aim through diverse isothermal and kinetic models for the estimation of the chosen antibiotic on adsorbent adsorption parameters.

## 2. Methodology and Materials

**2.1. Reagents and Chemicals.** Calcium chloride dihydrate (CaCl<sub>2</sub>·2H<sub>2</sub>O) was bought to be available and of an analytical grade from AVONCHEM, UK; ferric nitrate (Fe(NO<sub>3</sub>)<sub>3</sub>·9H<sub>2</sub>O) from Scharlau, Spain; and sodium alginate powder (food grade, China) with a 2.5 × 10<sup>5</sup> g/mol molecular. Also, sodium hydroxide (NaOH) from Alpha Chemika, India, and hydrochloric acid (HCl, 35-38% pure) were also bought from CDH, India, and were used in this work. We used amoxicillin powder (C<sub>16</sub>H<sub>19</sub>N<sub>3</sub>O<sub>5</sub>S) with purity: 97.5% from the general drug company in Samarra, Iraq, specifically, the antibiotic chosen in this work in order to simulate contamination within the studied groundwater and used in experiments without any further purification. During batch experiments, we prepared one liter of aqueous solution with a 1000 mg contamination and kept at room temperature, and the dilution of stock solution was conducted

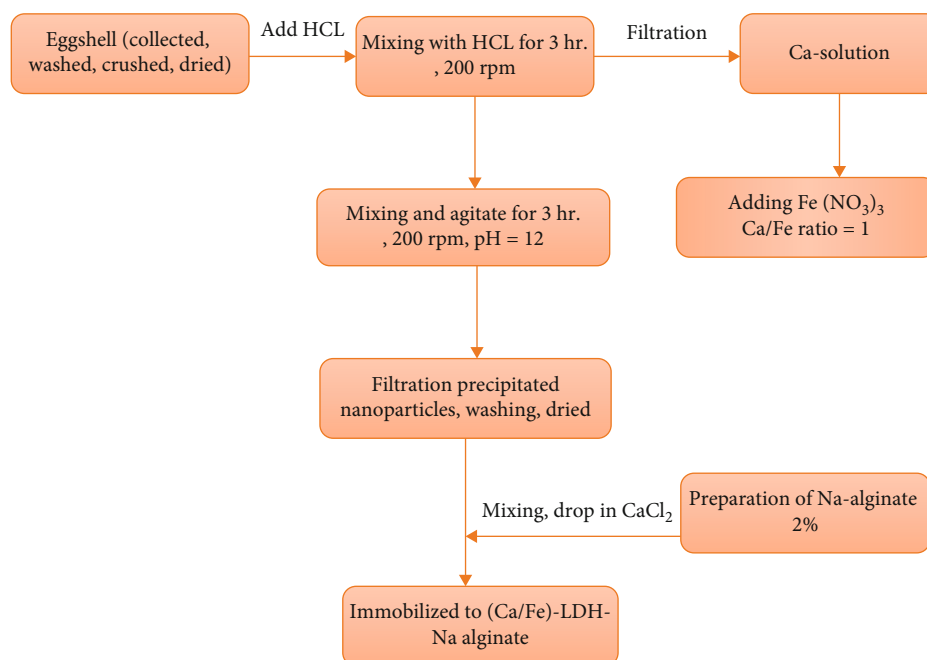


FIGURE 1: Flowchart of preparing (Ca/Fe)-LDH-SA beads.

with distilled deionized water for obtaining the required target contaminant solution concentration.

2.2. *Synthesizing (Ca/Fe)-LDH-SA Beads.* The main concept used in synthesizing (Ca/Fe)-LDH adsorbent as in Figure 1 involves five steps illustrated below:

- (1) From chicken eggshells, calcium ions are extracted, which gathering from household wastes, requiring mixing 20 gram of crushed and dried shells (after collecting from the source, rinsing with water several times, air-drying, crushing, drying at 105°C, passing on sieving for gaining (0.6 mm) are shown in Figure 2, then adding 100 mL of solution made of distilled water and 10 mL from 35–38% hydrochloric acid to prepare mixture stirred vigorously at room temperature for 3 h at 200 rpm. To obtain a clear calcium solution, the residual solid shell particles can be separated using filter paper from the calcium ion-rich aqueous solution
- (2) Preparing aqueous solution reached with  $\text{Fe}^{+3}$  by dissolved specific mass of  $\text{Fe}(\text{NO}_2)_3$ . This dissolving process happened in distilled water (DW), then mixing this iron solution with the calcium ion-rich aqueous solution obtained from first step to obtain solution of (Ca/Fe) with molar ratio = 1
- (3) In flask, changing the alkalinity of the mixture by adding 1 M NaOH to reach a value of around 12 ensured forming (Ca/Fe)-LDH nanoparticles with continuous agitation over 3 hours and 200 rpm, and then, the slurry that formed should be filter on filter paper, collect it and wash it with distilled water,

and dry and grind to obtain the nanoparticles as a powder as shown in Figure 3.

- (4) Sodium alginate is made through the same procedure of previous studies [38]. This procedure involves dissolving 2 g Na-alginate in 100 mL of DW and comprehensively agitated through magnetic stirring at room ambient over twenty-four hours.

5. Adding the mass of (Ca/Fe) nanoparticles equal 5 g/100 mL (as optimum value obtained from [39]) that formed in the previous step for the sodium alginate introduced by 10 mL syringe into 0.1 M of  $\text{CaCl}_2$  (dissolving 1 g of  $\text{CaCl}_2$  in 100 mL DW) so that polymerization and beads are formed at 4 mm. They should cure in this solution for one hour and followed by washing it two times by DW and keeping it in 5 mM of  $\text{CaCl}_2$  (0.278 g of  $\text{CaCl}_2$  is dissolved in 500 mL DW) at 4°C for additional uses (Figure 4).

2.3. *Batch Methodology.* It is recommended that batch adsorption experiments be analysed using phenomenological models in order to obtain the appropriate values of operating conditions needed for removing the large percentage of adopted contaminant concentrations that are applicable to other systems and for reducing the number of experiments to fully describe the kinetics of adsorption, which is typically characterized on the basis of empirical models [40]. Some flasks of 250 mL were made, and simulated contaminated water (100 mL) is put in each flask with certain values of concentrations. We repeated experiments by changing variables to obtain important information about the behaviors of antibiotics sorption onto (Ca/Fe)-LDH-immobilized beads and the best parameters to remove it (primary pH, contact time, the amount of beads, and the speed of agitation or the initial concentration of the solution), for getting the



FIGURE 2: Eggshell (a) before and (b) after dried, crushed, and sieved.

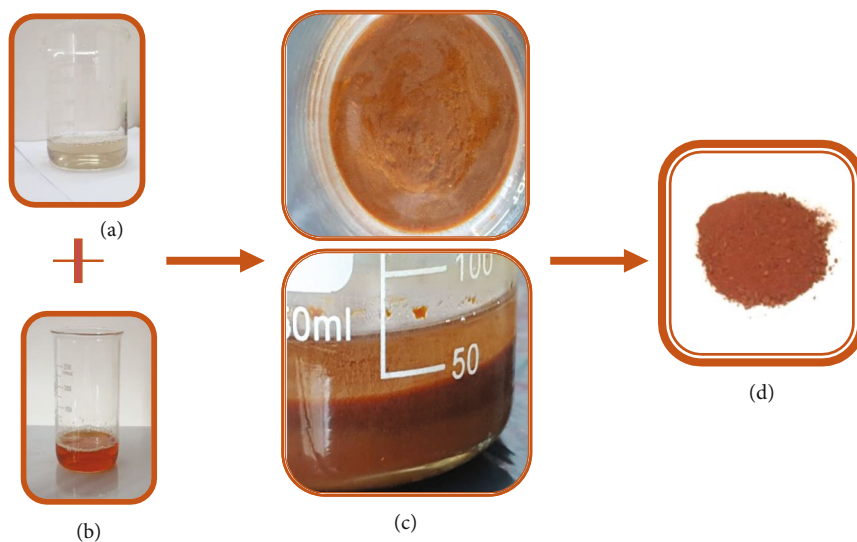


FIGURE 3: (a) Solution of extracted calcium; (b) iron solution; (c) after coprecipitation (Ca/Fe)-LDH; (d) (Ca/Fe)-LDH nanoparticles after filtration and drying.

isotherms and kinetics of adsorption at the end. Diverse concentration solutions of AMX were obtained from  $1000 \text{ mg} \cdot \text{L}^{-1}$  stock solution through dilution methods in different intervals of time for three hours. For adsorption kinetics, different initial concentrations of AMX, i.e., from  $100 \text{ mg} \cdot \text{L}^{-1}$  to  $250 \text{ mg} \cdot \text{L}^{-1}$  in  $100 \text{ mL}$  volume, are connected to  $0.5 \text{ g}$  of adsorbent beads. We examined pH on AMX adsorption in

range 2-12 where we adjusted pH of solutions by the NaOH and HCl solution, while the agitation speed did not exceed  $250 \text{ rpm}$ . While studying the isotherm, we added various masses of (Ca/Fe)-LDH-SA beads of  $0.10\text{-}1.2 \text{ g}$  to some flasks with  $100 \text{ mL}$  solution for everyone. We interpreted the adsorption isotherm data for various isotherm models. We used filter paper to separate the alginate beads from



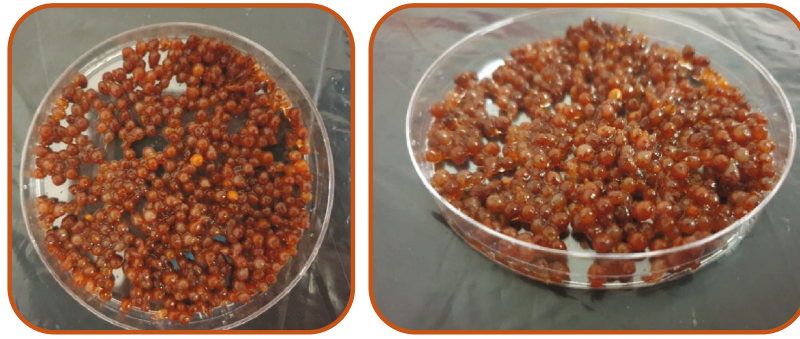


FIGURE 4: Beads of (Ca/Fe)-LDH-SA.

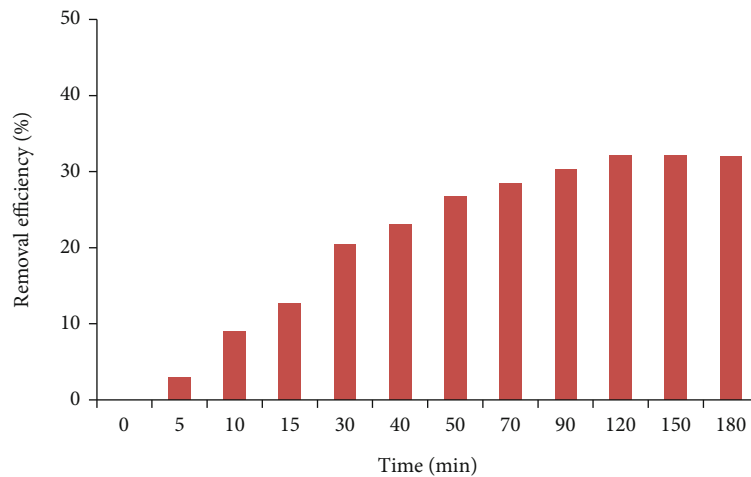


FIGURE 5: Contact time influence on the adsorbent bead behavior utilized to remove AMX from contaminated water.

the water and measured AMX antibiotic concentrations by ultraviolet-visible (UV) spectrophotometer (Model Varian Cary 100 conc., England) at wavelengths of 270 nm. Also, the mean for three readings of the sorption can be gained from each point.

2.4. Data Analysis. At the equilibrium ( $q_e$ ) according to the variance between initial concentration ( $C_o$ ) and final concentration ( $C_e$ ), Equation (1) is applied for the calculation of the quantity of antibiotics of the alginate beads at [41].

$$q_e = (C_o - C_e) \frac{V}{m}. \quad (1)$$

Here,  $m$  is the mass adsorbent beads in grams and  $V$  is the liter (L) volume of AMX solution, and we measured the antibiotics ( $R$ ) percentage that is removed from solution onto adsorbent by Equation (2) as in [42].

$$R = \frac{(C_o - C_e)}{C_o} \times 100. \quad (2)$$

### 3. Results and Discussion

3.1. Time Influence in Batch Testing. We identified the adsorption equilibrium time through the antibiotic concentra-

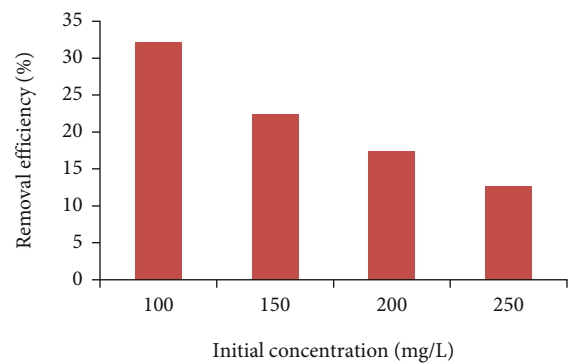


FIGURE 6: Effects of initial concentration on the adsorbent bead behavior used to remove AMX from contaminated water.

tions change with the time. Figure 5 is the change in the AMX uptake efficiencies from contaminated water onto the made adsorbent to contact time not more than three hours at operational settings of initial concentration ( $C_o$ ) = 100 mg/L, pH = 7, mass of beads = 0.5 g/100 mL, and speed of agitation = 200 rpm. We removed the antibiotic rapidly for initial times until balance is achieved, or complete absorption for reducing 30.3% AMX at one hours and a half when  $C_o$  100 mg/L is decreased after that time because of reducing binding sites

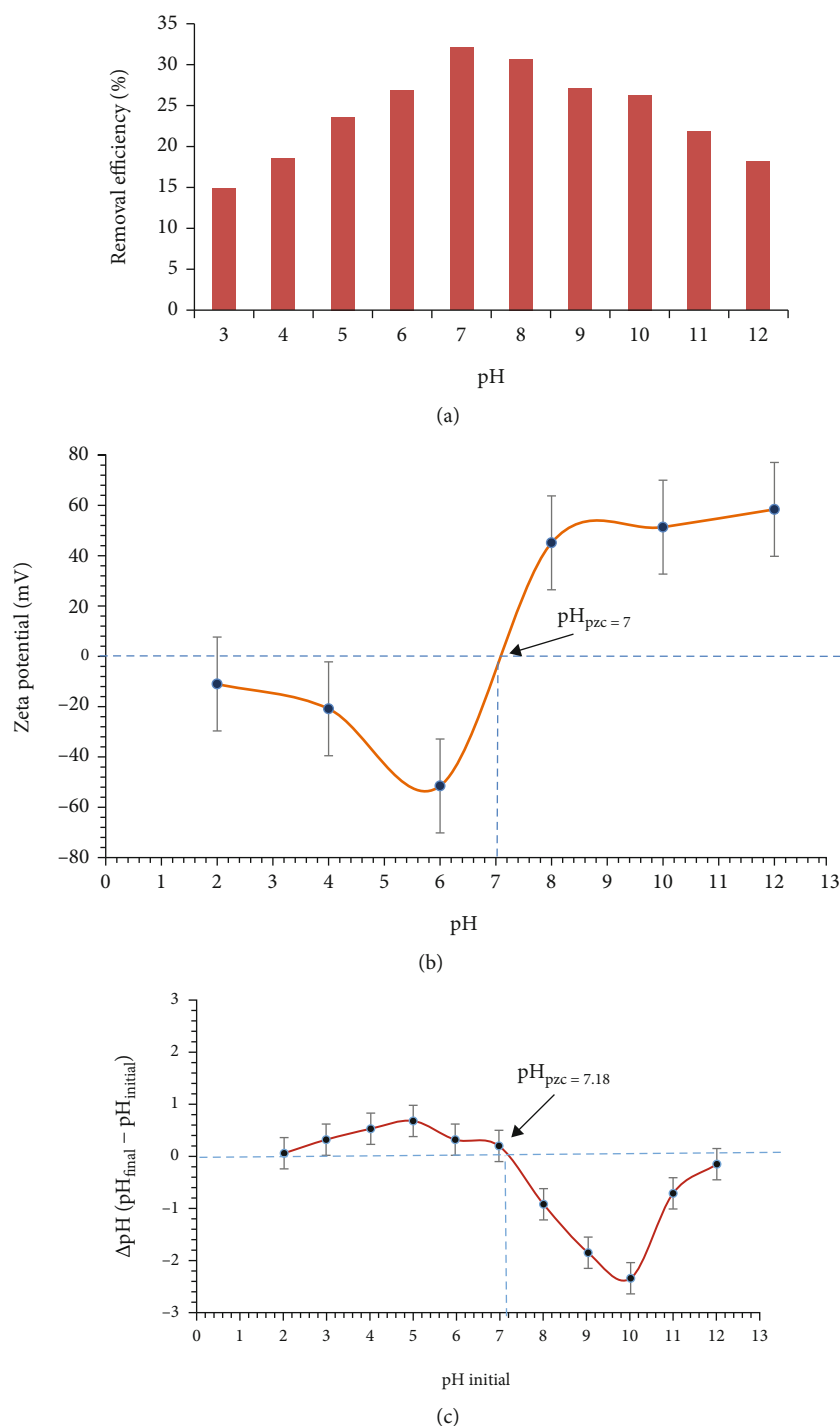


FIGURE 7: (a) Initial pH effect with removal of AMX from contaminated water, (b)  $pH_{pzc}$  for Ca/Fe LDH, and (c)  $pH_{pzc}$  of beads.

for AMX molecule sorption [43]. The increase in the adsorption time does not make the adsorption rate obviously change since the removal percentages had been slowly tended to be stable till 180 min because the quantity of free sites drops, and the binding of adsorbate from the aqueous solution is harder, and the sorption processes, thus, decreases [44].

**3.2. AMX Initial Concentration Influence.** According to Figure 6, the AMX antibiotic removing efficiencies onto syn-

thesized adsorbent beads decreased intensely from 32.1% for  $C_o$  100 mg/L to 12.72% for  $C_o$  250 mg/L at 90 min, pH 7, mass of beads 0.5 g/100 mL, and speed of agitation 200 rpm. With the existing binding sites, all contaminant molecules interacted at lesser concentrations causing a remarkable rise in the sorption efficiency. So, these contaminants sorbed per unit mass of adsorbent reduced with the rise in initial concentration based on the sites of the process which was less favorable sites with the decrease in the concentration [45]. Although

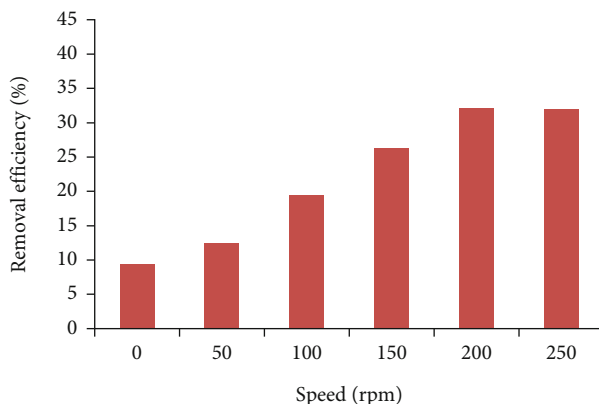


FIGURE 8: Effects of agitation speed on the behavior of adsorbent beads to remove AMX from contaminated water.

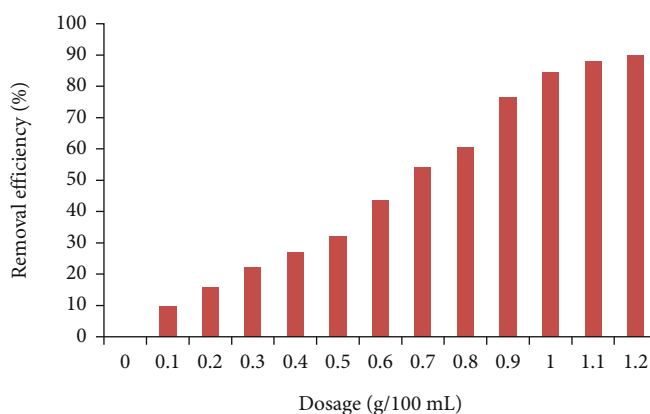


FIGURE 9: Relation between sorbent dosage and removals of AMX.

adsorbent removed all antibiotics at one and half hours under the same conditions, possibly, the antibiotic showed higher removal if the concentration was lower than the detecting limit as in environmental concentrations.

**3.3. Impacts of pH on Removal Efficiency of AMX.** The contaminated aqueous pH that contact with the synthesized adsorbent beads is important in eliminating antibiotic as this variable may influence the exterior charges of beads, the AMX ionization degree, and the dissociation of the functional groups [46]. Figure 7(a) is the plots of removing efficiencies of AMX versus various initial pH different from 3 to 12. The process of removing was low ( $\leq 14.9\%$  at pH 3.0) because antibiotic competes  $H^+$  ions. The rise of the pH towards the neutral condition is followed by a rise in the sorption effectiveness higher than 32.1% for the used antibiotics at pH 7. The antibiotic ionization and hydration decrease at neutral conditions, enhancing removal by the hydrogen bonds and  $\pi-\pi$  stacking influence. The figure also reveals a decrease in the removing efficiency because solution changed towards the basic form, and the AMX competences are bigger than 18.2%. This efficiency reduction with higher pH could be due to generating  $OH^-$  attenuating the hydrogen bonding. Figure 7(b) shows the  $pH_{pzc}$  of Ca/Fe-LDH at 7 and for beads calculated as around 7.18, and Figure 7(c) reveals a positive charge of the  $pH < pH_{pzc}$ , the

TABLE 1: Kinetic models for sorption of AMX antibiotic onto the synthesized nanoadsorbent.

Model	Parameter	Value
Pseudo-first-order	$q_e$ (mg/g)	3.2828
	$k_1$ ( $min^{-1}$ )	0.0298
	$R^2$	0.9899
	SSE	0.1554
Pseudo-second-order	$q_e$ (mg/g)	4.0288
	$k_2$ (g/mg min)	0.0077
	$R^2$	0.9924
	SSE	0.1287
Intraparticle diffusion	Portion 1	
	$k_{int}$ ( $mg/g \min^{0.5}$ )	0.3958
	$R^2$	0.9519
	Portion 2	
	$k_{int}$ ( $mg/g \min^{0.5}$ )	0.1431
	$R^2$	0.9615
	Portion 3	
	$k_{int}$ ( $mg/g \min^{0.5}$ )	0.0182
	$R^2$	0.6334

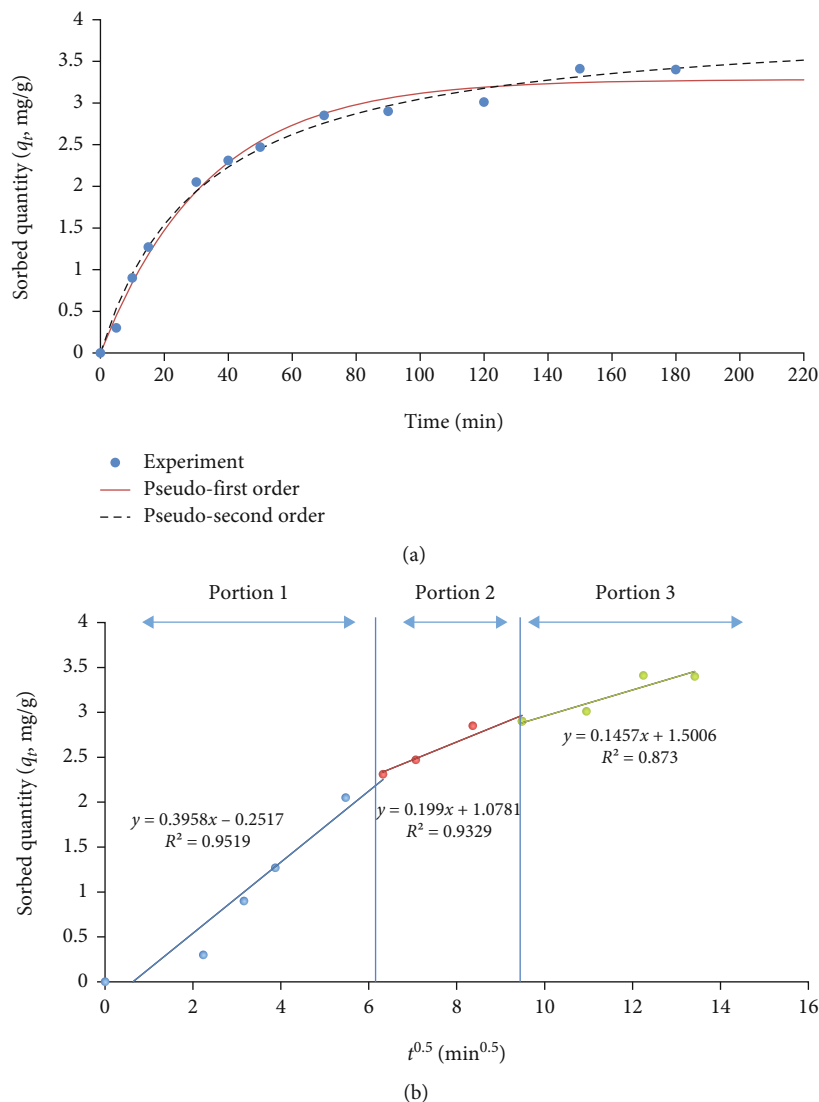


FIGURE 10: (a) Kinetic (b) and intraparticle diffusion models for interaction of sodium alginate beads with water-contained AMX.

adsorbent surface, and the negative one at  $\text{pH} > \text{pH}_{\text{pzc}}$ . As the initial pH rose, zeta potential significantly rose from range 2-6 with the AMX adsorption of onto Ca/Fe-LDH-Na-alginate beads. So, the adsorption of the AMX on bead at pH range 2-6 seemed to be low because electrostatic attraction AMX electrostatically attracts bead surface which confirm well the results above. So, at higher pH ( $6 < \text{pH} < 8$ ), AMX on the adsorbent did not leak our acting as the adsorption sites for AMX. So, the reduction in the AMX and bead reaction caused a higher adsorption of AMX. While the pH rose more, the adsorption capacity reduced, so we conducted other AMX adsorption experiments at pH 7.

**3.4. Influence of Agitation Speed.** The agitation percentage influenced highly that of adsorption which rises when the speed of agitation rises. According to Figure 8, the increase in agitation speed is essential to enhance AMX removal from polluted water because of diffusion rate of AMX molecules

TABLE 2: Isotherm model parameters in the AMX sorption onto adsorbent beads.

Model	Parameter	Value
Langmuir	$q_{\text{max}}$ (mg/g)	6.7362
	$b$ (L/mg)	0.2077
	$R^2$	0.9467
	SSE	1.35814
Freundlich	$K_f$ (mg/g)(L/mg) $^{1/n}$	3.32892
	$n$	7.96808
	$R^2$	0.622078
	SSE	9.30767

that rise towards the adsorbent bead surface under operational parameters of time = 90 min, pH = 7, 0.5 g/100 mL beads mass, and primary adsorbate = 100 mg/L concentration. Removing AMX efficiencies was not bigger than 9.4%



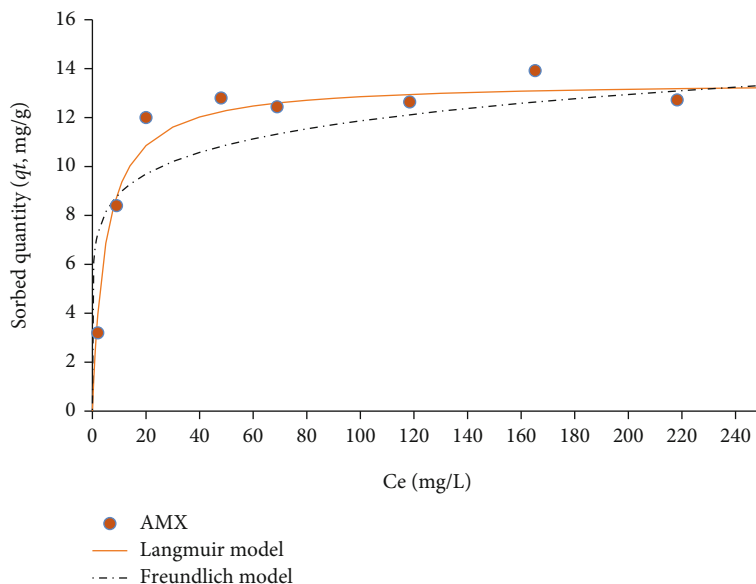


FIGURE 11: Sorption isotherms for interaction of designed sorbent—AMX water contaminated.

for static aqueous solutions, although dramatically rose at 32.1% at 200 rpm. Yet, the figure also explains that the adsorption rises when agitation speeds rise only up to a specific limit, so speed to 250 rpm increase does not make any changes in the removal efficiencies because beyond, there is no rise in the adsorption capacity [47].

**3.5. Adsorbent Alginate Bead Mass Impacts.** Figure 9 shows the adsorbent alginate beads mass effect on removing AMX efficiencies. Thus, when the dosage changes from 0.1 to 1.2 g, the removing efficiencies increase from the least (9.8%) to more than 90% for the used antibiotic. The bead quantity rise indicates a growth in the empty sites ready to interact with contaminant molecules leading to increase the removing efficiencies of these molecules [48].

**3.6. Kinetics of Antibiotic Sorption.** Adsorption kinetics from batch study is one of the most important features of such processes that control the sorbent's capacity for adsorption and rate of adsorption at the interface of solid-liquid phases due to the equilibrium state in batch mode, and the kinetics helps researchers who conducted laboratory scale research to estimate an adsorbent's performance before applying it on a larger scale [49]. This work measures the kinetic data in the experiment by kinetic models; pseudo-first-order and pseudo-second-order models are shown in Equations (3) and (4), respectively, and intraparticle diffusion model is shown in Equation (5) [50–52]:

$$q_t = q_e \left( 1 - e^{-k_1 t} \right), \quad (3)$$

$$q_t = \frac{k_2 q_e^2 t}{(1 + k_2 q_e t)}, \quad (4)$$

$$q_t = k_{\text{int}} t^{0.5} + C. \quad (5)$$

Here,  $q_e$  is the solid matrix at equilibrium and  $q_t$  is the time which the quantities of pollutant were adsorbed in mg/g,  $k_1$  refers to the pseudo first order model rate constant (1/min),  $k_2$  stands for the sorption (g/mg min) rate constant, and  $k_{\text{int}}$  is the sorption rate constant of for this model (mg/g min<sup>0.5</sup>);  $C$  is the intercept. We used kinetic models for formulating the sorption of the antibiotic AMX over time by alginate beads for various initial pollutant concentration. We also used Excel 2016's "Solver" nonlinear regression feature for completing the formulation process. Table 1 is the parameters for kinetic models determined by fitting, confirming the second model AMX interaction represented by alginate because of the determination coefficient ( $R^2$ ) which is bigger than 0.9924, and squared error sum (SSE) is lower than 0.1287. Also, from Figure 10(a), the calculated AMX sorbed quantity onto the alginate beads at 4.0288 mg/g, nearly approaching the calculated quantity as a sign for the second order model applicability. So, the AMX sorption onto alginate beads happened through the chemisorption (i.e., chemical reaction). The study used the intraparticle diffusion (Equation (5)) model and the equation of constants between  $q_t$  and  $t^{0.5}$  in measuring nonlinear regression fitting (Table 1). Figure 10(b) shows this relationship for the investigated antibiotic represented through the straight lines with intercept not equal to zero. Thus, intraparticle diffusion needs the AMX sorption with no depiction of the rate-controlling step [53]. This is a multilinearity plot, meaning it is two or more simultaneous methods in the AMX sorption. So, the line slope in "portion 1" is sharp; so, removing contaminant rates could increase in the primary sorption because of the external surface adsorption caused by the existing vacant site. The line slope in the "portion 2" changed gradually to the intraparticle diffusion possibly rate-controlled. At the end, the "portion 3" is the equilibrium stage connected to the diffusion reducing the speed because of low remaining contaminant concentration in the liquid [54–56].

**3.7. Isotherms for Equilibrium Sorption Readings.** Adsorption is, in general, conducted by equilibrium isotherm relationship correlating between the solute-sorbed quantity on the solid materials ( $q_e$ , mg/g) and its concentration ( $C_e$ , mg/L) staying in the aqueous solution at certain temperatures. So, there could be an increase in the solute which removed solid particle per unit mass because of the rise in the concentration yet not directly [57]. An isotherm is possibly recognized “favorable” if the convex is upward due to the high loading that could occur the solid particles if the concentrations are low in the water phases [58]. The relationships described that the sorption isotherms are divided into Freundlich and Langmuir models.

For heterogeneous sites, Freundlich model can be applied with sorption in a multilayer scheme [59].

$$q_e = K_F C_e^{1/n}. \quad (6)$$

Langmuir model suits single-layer adsorption [60]:

$$q_e = \frac{q_{\max} b C_e}{1 + b C_e}, \quad (7)$$

where  $K_F$  is linked to the maximum adsorption capacity,  $1/n$  refers to the sorption intensity,  $b$  is the solute affinity with solid phases (L/mg), and  $q_{\max}$  is the highest sorption (mg/g). We calculated any constants in the used isotherm models as Table 2 shows by nonlinear regression by applying “solver” option in Excel software 2016. According to the  $R^2$  and SSE, Langmuir model stated that the AMX sorption depiction is made on adsorbent beads. The experimental measurement matching with the sorption isotherms is observed from Figure 11; yet, this is recognized from highest  $R^2$  ( $\geq 6.7362$ ) and lowest SSE ( $\leq 1.35814$ ). The AMX sorption maximum ability is 6.7362 mg/g, meaning that the alginate beads showed capability in the AMX removal. Freundlich constant ( $K_f$ ) reached 3.32892 (mg/g) (L/mg) $^{1/n}$  for AMX onto Na-alginate while ( $n$ )  $> 1$ ; so, the isotherm curves could be “favorable.”

## 4. Conclusions

In this study, egg shell waste was used as crucial source of calcium ions to synthesize a nanobiosorbent from calcium and iron and immobilized into alginate to formed (Ca/Fe)-LDH-SA beads and studied the relevance of using it as a reactive material in permeable barrier utilized for removing AMX from aqueous solution. This works confirmed the AMX antibiotic efficiency in removal from solution through the sorbent. The AMX sorption was explored the time function and primary concentration of AMX, pH of AMX, and sorbent dosage. The equilibrium time for the removal of AMX on adsorbent beads was achieved over one and a half hours and maximum removed at pH = (7). Based on the results, the appropriate operational settings need for assuring the efficacy of removing AMX  $\geq 95\%$  were 1.2 g/100 mL dosage for  $C_0$  100 mg/L at 200 rpm. Langmuir adsorption isotherm explained the adsorption isotherm data. Also,

chemical forces (i.e., chemisorption) governed this process because of applying the pseudo-second-order model, so the adsorbent was effective in removing chosen pollutant, and its utilization could be expanded to other antibiotics too. So, the manufactured (Ca/Fe)-LDH-SA beads could be competent in the permeable technology adsorption barrier and suitable in the fixed bed columns in removing AMX from water.

## Data Availability

All the available data are incorporated in the MS.

## Conflicts of Interest

No known personal relationships and competing financial interests are influencing this paper.

## References

- [1] P. Li, D. Karunanidhi, T. Subramani, and K. Srinivasamoorthy, “Sources and consequences of groundwater contamination,” *Archives of Environmental Contamination and Toxicology*, vol. 80, no. 1, pp. 1–10, 2021.
- [2] R. Thiruvengkatachari, S. Vigneswaran, and R. Naidu, “Permeable reactive barrier for groundwater remediation,” *Journal of Industrial and Engineering Chemistry*, vol. 14, no. 2, pp. 145–156, 2008.
- [3] UK Environmental Agency, 2005, <http://www.environment-agency.gov.uk/>.
- [4] S. S. D. Foster, *Groundwater-Past Achievements and Future Challenges*, O. Sililo, Ed., Balkema, Rotterdam, The Netherlands, 2000.
- [5] P. Bayer and M. Finkel, “Life cycle assessment of active and passive groundwater remediation technologies,” *Journal of Contaminant Hydrology*, vol. 83, no. 3-4, pp. 171–199, 2006.
- [6] USEPA, *Evaluation of Groundwater Extraction Remedies: Phase II, vol. 1, Summary Report, Publication 9355.4-05*, EPA Office of Emergency and Remedial Responses, Washington, DC, 1992.
- [7] P. Li and J. Wu, “Sustainable living with risks: meeting the challenges,” *Human and Ecological Risk Assessment: An International Journal*, vol. 25, no. 1-2, pp. 1–10, 2019.
- [8] M. Lu, Y. Y. Chen, M. Chiou, M. Y. Chen, and H. Fan, “Occurrence and treatment efficiency of pharmaceuticals in landfill leachates,” *Waste Management*, vol. 55, pp. 257–264, 2016.
- [9] R. S. Singer, R. Finch, H. C. Wegener, R. Bywater, J. Walters, and M. Lipsitch, “Antibiotic resistance—the interplay between antibiotic use in animals and human beings,” *The Lancet Infectious Diseases*, vol. 3, no. 1, pp. 47–51, 2003.
- [10] K. Kümmerer, “Significance of antibiotics in the environment,” *Journal of Antimicrobial Chemotherapy*, vol. 52, pp. 5–7, 2003.
- [11] WHO, *Overcoming antibiotic resistance, World Health Organization Report in Infectious Diseases*, WHO, Geneva, 2002.
- [12] A. K. Sarmah, M. T. Meyer, and A. Boxall, “A global perspective on the use, sales, exposure pathways, occurrence, fate and effects of veterinary antibiotics (VAs) in the environment,” *Chemosphere*, vol. 65, no. 5, pp. 725–759, 2006.
- [13] K. D. Brown, J. Kulis, B. Thomson, T. H. Chapman, and D. B. Mawhinney, “Occurrence of antibiotics in hospital, residential,

- and dairy effluent, municipal wastewater, and the Rio Grande in New Mexico,” *Science of the Total Environment*, vol. 366, no. 2–3, pp. 772–783, 2006.
- [14] C. Suarez and F. Gudiol, “Beta-lactam antibiotics,” *Enfermedades Infecciosas Y Microbiología Clínica*, vol. 27, no. 2, pp. 116–129, 2009.
- [15] M. Larramendy and S. Soloneski, Eds., *Environmental Health Risk: Hazardous Factors to Living Species*, BoD-Books on Demand, 2016.
- [16] R. Andreozzi, V. Caprio, C. Ciniglia et al., “Antibiotics in the environment: occurrence in Italian STPs, fate, and preliminary assessment on algal toxicity of amoxicillin,” *Environmental Science & Technology*, vol. 38, no. 24, pp. 6832–6838, 2004.
- [17] M. A. Carey, B. A. Fretwell, N. G. Mosley, and J. W. N. Smith, “Guidance on the use of permeable reactive barriers for remediating contaminated groundwater,” in *National Groundwater and Contaminated Land Centre Report NC/01/51*, Bristol, UK Environment Agency, 2002.
- [18] Y. Chen, J. Li, C. Lei, and H. Shim, “Interactions between BTEX, TPH, and TCE during their bio-removal from the artificially contaminated water,” in *Bionature 2011: The Second International Conference on Bioenvironment*, pp. 33–37, Biodiversity and Renewable Energies, Venice, Italy, 2011.
- [19] B. V. Babu and S. Gupta, “Adsorption of Cr(VI) using activated neem leaves: kinetic studies,” *Adsorption*, vol. 14, no. 1, pp. 85–92, 2008.
- [20] H. Parab, S. Joshi, N. Shenoy, A. Lali, U. S. Sarma, and M. Sudersanan, “Determination of kinetic and equilibrium parameters of the batch adsorption of Co(II), Cr(III) and Ni(II) onto coir pith,” *Process Biochemistry*, vol. 41, no. 3, pp. 609–615, 2006.
- [21] G. Regmi, B. Indraratna, L. D. Nghiem, A. N. Golab, and B. G. Prasad, “Treatment of acidic groundwater in acid sulfate soil terrain using recycled concrete: column experiments,” *Journal of Environmental Engineering, ASCE*, vol. 137, no. 6, pp. 433–443, 2011.
- [22] S. G. Benner, D. W. Blowes, C. J. Ptacek, and K. U. Mayer, “Rates of sulfate reduction and metal sulfide precipitation in a permeable reactive barrier,” *Applied Geochemistry*, vol. 17, no. 3, pp. 301–320, 2002.
- [23] P. K. Mondal, G. Lima, D. Zhang et al., “Evaluation of peat and sawdust as permeable reactive barrier materials for stimulating in situ biodegradation of trichloroethene,” *Journal of Hazardous Materials*, vol. 313, pp. 37–48, 2016.
- [24] S. K. Mahmood, G. A. Sultan, S. K. Ebrahim, and A. G. M. Alhaaik, “Recycling of chicken egg shells into nanopowder: synthesis, and its properties,” *Baghdad Science Journal*, vol. 19, pp. 0759–0759, 2022.
- [25] H. Faridi and A. Arabhosseini, “Application of eggshell wastes as valuable and utilizable products: a review,” *Research in Agricultural Engineering*, vol. 64, no. 2, pp. 104–114, 2018.
- [26] A. Laca, A. Laca, and M. Díaz, “Eggshell waste as catalyst: a review,” *Journal of Environmental Management*, vol. 197, pp. 351–359, 2017.
- [27] D. A. Oliveira, P. Benelli, and E. R. Amante, “A literature review on adding value to solid residues: egg shells,” *Journal of Cleaner Production*, vol. 46, pp. 42–47, 2013.
- [28] H. B. Lakshmi, B. J. Madhu, and M. Veerabhadraswamy, “Synthesis and characterization of nano-crystalline CaFe<sub>2</sub>O<sub>4</sub> via solution combustion method from solid waste egg shells as source of calcium,” *International Journal of Engineering Research And Advanced Technology*, vol. 3, pp. 21–30, 2017.
- [29] J. Carvalho, J. Araujo, and F. Castro, “Alternative low-cost adsorbent for water and wastewater decontamination derived from eggshell waste: an overview,” *Waste and Biomass Valorization*, vol. 2, no. 2, pp. 157–167, 2011.
- [30] A. Q. Muryoush, D. Hussain, and A. H. Ali, “Antibacterial activity with eggshell nano-particles activated by microwave plasma,” *Journal of Optoelectronic and Biomedical Materials*, vol. 13, no. 4, pp. 177–182, 2021.
- [31] S. N. Ishak and N. A. N. N. Malek, “Functionalized layered double hydroxide with compound to remove cationic and anionic pollutants: a review,” *Environmental and Toxicology Management*, vol. 1, no. 1, pp. 26–29, 2021.
- [32] X. Wang, H. Zhao, L. Chang et al., “First-principles study on interlayer spacing and structure stability of NiAl-layered double hydroxides,” *ACS Omega*, vol. 7, no. 43, pp. 39169–39180, 2022.
- [33] M. N. Sepehr, T. J. Al-Musawi, E. Ghahramani, H. Kazemian, and M. Zarrabi, “Adsorption performance of magnesium/aluminum layered double hydroxide nanoparticles for metronidazole from aqueous solution,” *Arabian Journal of Chemistry*, vol. 10, no. 5, pp. 611–623, 2017.
- [34] Y. Kuang, L. Zhao, S. Zhang, F. Zhang, M. Dong, and S. Xu, “Morphologies, preparations and applications of layered double hydroxide micro-/nanostructures,” *Materials*, vol. 3, no. 12, pp. 5220–5235, 2010.
- [35] I. N. Abd and M. J. Mohammed-Ridha, “Simultaneous adsorption of tetracycline and amoxicillin by cladophora and spirulina algae biomass,” *Iraqi Journal of Agricultural Sciences*, vol. 52, no. 5, pp. 1290–1303, 2021.
- [36] C. Yang, L. Wang, Y. Yu et al., “Highly efficient removal of amoxicillin from water by Mg-Al layered double hydroxide/cellulose nanocomposite beads synthesized through in-situ coprecipitation method,” *International Journal of Biological Macromolecules*, vol. 149, pp. 93–100, 2020.
- [37] A. Elhaci, F. Labeled, A. Khenifi, Z. Bouberka, M. Kameche, and K. Benabbou, “MgAl-layered double hydroxide for amoxicillin removal from aqueous media,” *International Journal of Environmental Analytical Chemistry*, vol. 101, no. 15, pp. 2876–2898, 2021.
- [38] M. Y. Arica, Y. Kacar, and Ö. Genç, “Entrapment of white-rot fungus *Trametes versicolor* in Ca-alginate beads: preparation and biosorption kinetic analysis for cadmium removal from an aqueous solution,” *Bioresource Technology*, vol. 80, no. 2, pp. 121–129, 2001.
- [39] M. F. Abed and A. A. Faisal, “Calcium/iron-layered double hydroxides-sodium alginate for removal of tetracycline antibiotic from aqueous solution,” *Alexandria Engineering Journal*, vol. 63, pp. 127–142, 2023.
- [40] V. P. Mulgundmath, R. A. Jones, F. H. Tezel, and J. Thibault, “Fixed bed adsorption for the removal of carbon dioxide from nitrogen: breakthrough behaviour and modelling for heat and mass transfer,” *Separation and Purification Technology*, vol. 85, pp. 17–27, 2012.
- [41] Y. Wang, S. Gong, Y. Li, Z. Li, and J. Fu, “Adsorptive removal of tetracycline by sustainable ceramsite substrate from bentonite/red mud/pine sawdust,” *Scientific Reports*, vol. 10, no. 1, pp. 1–18, 2020.
- [42] P. Das, P. Debnath, and A. Debnath, “Enhanced sono-assisted adsorptive uptake of malachite green dye onto magnesium ferrite nanoparticles: kinetic, isotherm and cost analysis,” *Environmental Nanotechnology, Monitoring & Management*, vol. 16, article 100506, 2021.

- [43] A. A. H. Faisal and L. A. Najji, "Simulation of ammonia nitrogen removal from simulated wastewater by sorption onto waste foundry sand using artificial neural network," *Association of Arab Universities Journal of Engineering Sciences*, vol. 26, pp. 28–34, 2019.
- [44] A. R. Lucaci, D. Bulgariu, and L. Bulgariu, "In situ functionalization of iron oxide particles with alginate: a promising biosorbent for retention of metal ions," *Polymers*, vol. 13, no. 20, p. 3554, 2021.
- [45] Z. T. Abd Ali, M. A. Ibrahim, and H. M. Madhloom, "Eggshell powder as an adsorbent for removal of Cu (II) and Cd (II) from aqueous solution: equilibrium, kinetic and thermodynamic studies," *Al-Nahrain Journal for Engineering Sciences*, vol. 19, no. 2, pp. 186–193, 2016.
- [46] M. Wawrzekiewicz and Z. Hubicki, "Removal of tartrazine from aqueous solutions by strongly basic polystyrene anion exchange resins," *Journal of Hazardous Materials*, vol. 164, no. 2–3, pp. 502–509, 2009.
- [47] H. A. Ihsanullah Asmaly, T. A. Saleh, T. Laoui, V. Kumar Gupta, and M. A. Atieh, "Enhanced adsorption of phenols from liquids by aluminum oxide/carbon nanotubes: comprehensive study from synthesis to surface properties," *Journal of Molecular Liquids*, vol. 206, pp. 176–182, 2015.
- [48] L. Wei, F. Zietzschmann, L. C. Rietveld, and D. Van Halem, "Fluoride removal by Ca-Al-CO<sub>3</sub> layered double hydroxides at environmentally-relevant concentrations," *Chemosphere*, vol. 243, article 125307, 2020.
- [49] B. Debnath, M. Majumdar, M. Bhowmik, K. L. Bhowmik, A. Debnath, and D. N. Roy, "The effective adsorption of tetracycline onto zirconia nanoparticles synthesized by novel microbial green technology," *Journal of Environmental Management*, vol. 261, article 110235, 2020.
- [50] S. Lagergren, "About the theory of so-called adsorption of soluble substances, K. seventeen," *The Hand*, vol. 24, pp. 1–39, 1989.
- [51] Y. S. Ho and G. McKay, "Pseudo-second order model for sorption processes," *Process Biochemistry*, vol. 34, no. 5, pp. 451–465, 1999.
- [52] S. Srivastava, R. Tyagi, and N. Pant, "Adsorption of heavy metal ions on carbonaceous material developed from the waste slurry generated in local fertilizer plants," *Water Research*, vol. 23, no. 9, pp. 1161–1165, 1989.
- [53] F.-C. Wu, R.-L. Tseng, and R.-S. Juang, "Comparisons of porous and adsorption properties of carbons activated by steam and KOH," *Journal of Colloid and Interface Science*, vol. 283, no. 1, pp. 49–56, 2005.
- [54] A. Özer, G. Gürbüz, A. Çalimli, and B. K. Körbahti, "Biosorption of copper(II) ions on *Enteromorpha prolifera*: application of response surface methodology (RSM)," *Chemical Engineering Journal*, vol. 146, no. 3, pp. 377–387, 2009.
- [55] L. Wang, J. Zhang, R. Zhao, Y. Li, C. Li, and C. Zhang, "Adsorption of Pb(II) on activated carbon prepared from *Polygonum orientale* Linn.: kinetics, isotherms, pH, and ionic strength studies," *Bioresource Technology*, vol. 101, no. 15, pp. 5808–5814, 2010.
- [56] W. H. Cheung, Y. S. Szeto, and G. McKay, "Intraparticle diffusion processes during acid dye adsorption onto chitosan," *Bioresource Technology*, vol. 98, no. 15, pp. 2897–2904, 2007.
- [57] R. H. Perry and C. H. Chilton, *Chemical Engineers' Handbook*, pp. 10–46, McGraw-Hill Book Company, 1984.
- [58] L. Warren and P. Harriott, *Unit Operation of Chemical Engineering*, McGraw-Hill Publ. Co, 1995.
- [59] Y. S. Ho, J. F. Porter, and G. McKay, "Equilibrium isotherm studies for the sorption of divalent metal ions onto peat: copper, nickel and lead single component systems," *Water, Air, and Soil Pollution*, vol. 141, pp. 1–33, 2002.
- [60] K. Y. Foo and B. H. Hameed, "Insights into the modeling of adsorption isotherm systems," *Chemical Engineering Journal*, vol. 156, no. 1, pp. 2–10, 2010.